ARTICLE IN PRESS

Available online at www.sciencedirect.com

ScienceDirect

Journal of Computational and Applied Mathematics ▮▮▮ (▮▮▮▮) ▮▮▮–▮▮▮

JOURNAL OF COMPUTATIONAL AND APPLIED MATHEMATICS

www.elsevier.com/locate/cam

On the numerical solution of diffusion–reaction equations with singular source terms

M. Ashyraliyev*, J.G. Blom, J.G. Verwer

CWI, P.O. Box 94079, 1090 GB Amsterdam, The Netherlands

Received 4 October 2006; received in revised form 11 April 2007

Abstract

A numerical study is presented of reaction–diffusion problems having singular reaction source terms, singular in the sense that within the spatial domain the source is defined by a Dirac delta function expression on a lower dimensional surface. A consequence is that solutions will be continuous, but not continuously differentiable. This lack of smoothness and the lower dimensional surface form an obstacle for numerical discretization, including amongst others order reduction. In this paper the standard finite volume approach is studied for which reduction from order two to order one occurs. A local grid refinement technique is discussed which overcomes the reduction.

MSC: primary 65M12;65M20; 65L05

Keywords: Reaction–diffusion equations; Singular source terms; Finite volume methods

1. Introduction

In this paper we discuss the numerical solution of diffusion–reaction problems

$$u_t = L(u) + f \tag{1.1}$$

with a singular reaction source term f. Singular means here that within the domain $\Omega \subset \mathbb{R}^d$ of L the source f is defined by a Dirac delta function expression on a lower dimensional surface $\Gamma \subset \Omega$ rather than on the whole of Ω. A consequence is that the solution u is not a solution on Ω in the classical sense because across Γ the solution u will be continuous, but not continuously differentiable. This lack of smoothness and the lower dimension of Γ form an obstacle for numerical discretization. With any numerical method one has the obvious question how to represent Γ and how to discretize f on a common grid. For finite-difference methods this question is studied in detail in [8] using regularization ideas. Regularization in the sense that the Dirac delta function expression is approximated by a source giving a small but regular support allowing standard finite difference schemes for L. In a close vicinity of Γ the lack of smoothness of u will still be felt with regularization, in the sense that in general the convergence order in the maximum norm is at best equal to one [8].

* Corresponding author.
E-mail address: M.Ashyraliyev@cwi.nl (M. Ashyraliyev).

0377-0427/$ - see front matter © 2007 Elsevier B.V. All rights reserved.
doi:10.1016/j.cam.2007.04.017

In this paper we follow the finite volume approach based on the integral form of (1.1). We consider this approach more natural than the finite difference one directly based on the differential form, since for the integral form the treatment of the Dirac delta function expression is mathematically clear. However, also with the finite volume approach on the uniform grid the problem of lack of smoothness remains, causing order reduction from two to one for the standard second-order spatial discretization scheme. To reobtain second-order convergence we examine the finite volume approach on special locally refined grids.

The paper is organized as follows. In Section 2 we study the standard finite volume discretization on a uniform grid for linear and nonlinear test models. We start with linear 1D and 2D test models where the emphasis lies on boundary value problems. These test models are simple but yet significant enough to reveal the essence of a singular source. Further, we turn our attention to initial-boundary value problems having nonlinear source terms. In Section 3 we study the finite volume approach on a locally refined grid for 1D and 2D linear test models. The paper is concluded with remarks in Section 4.

2. The finite volume approach on the uniform grid

2.1. The 1D boundary value problem

We begin with the boundary value problem for the 1D equation

$$-u_{xx} = \phi(x), \quad 0 < x < 1, \tag{2.1}$$

provided with the homogeneous Dirichlet conditions $u(0) = 0$, $u(1) = 0$. This simple 1D problem provides a nice test model. In spite of its simplicity it already reveals essential numerical properties for the Dirac delta function source $\phi(x) = \delta(x - \bar{x})$, $\bar{x} \in (0, 1)$. For this ϕ the solution u of (2.1) is no longer a classical solution in the sense that it can be explicitly substituted in the differential equation. It can be determined, however, by Green's function expression [1]

$$u(x) = \int_0^1 G(x, y)\phi(y)\,\mathrm{d}y, \quad G(x, y) = \begin{cases} x(1 - y), & 0 \leqslant x \leqslant y, \\ y(1 - x), & y < x \leqslant 1. \end{cases} \tag{2.2}$$

Using the delta function property $\int_0^1 f(x)\delta(x - \bar{x}) = f(\bar{x})$, insertion of $\phi(x) = \delta(x - \bar{x})$ gives

$$u(x) = \begin{cases} x(1 - \bar{x}), & 0 \leqslant x \leqslant \bar{x}, \\ \bar{x}(1 - x), & \bar{x} < x \leqslant 1. \end{cases} \tag{2.3}$$

Note that u is continuous but not continuously differentiable over [0, 1].

In this section we will analyze the standard cell-centered discretization scheme for (2.1) obtained through the finite volume approach. For u smooth (sufficiently differentiable) this scheme converges with second order in the maximum norm. However, for the solution defined by the Dirac delta function the scheme becomes locally inconsistent near $\bar{x}$ resulting in a maximum norm order reduction from two to one for the global error. For the sake of insight we will analyze this reduction phenomenon from two points of view, viz. by introducing modified equations as in backward error analysis and by examining the local truncation error as in common (forward) error analysis.

Let $h = 1/N$ where N is the number of uniform grid cells $\Omega_i = [(i - 1)h, ih]$ for $i = 1, \ldots, N$ covering [0, 1]. Let $x_i = (i - 1/2)h$ denote the cell center of Ω_i. The finite volume approach for (2.1) amounts to first integrating (2.1) over Ω_i and dividing by the cell volume,

$$\frac{\int_{\Omega_i} -u_{xx}(x)\,\mathrm{d}x}{\int_{\Omega_i} \mathrm{d}x} = \frac{\int_{\Omega_i} \phi(x)\,\mathrm{d}x}{\int_{\Omega_i} \mathrm{d}x}, \quad i = 1, \ldots, N,$$

followed by applying the divergence (Gauss) theorem,

$$-\frac{u_x(x_{i+1/2})}{\int_{\Omega_i} \mathrm{d}x} + \frac{u_x(x_{i-1/2})}{\int_{\Omega_i} \mathrm{d}x} = \frac{\int_{\Omega_i} \phi(x)\,\mathrm{d}x}{\int_{\Omega_i} \mathrm{d}x}, \quad i = 1, \ldots, N, \tag{2.4}$$

followed by choosing a difference approximation for u_x and computing the integrals, either exact or by a quadrature rule. After incorporating the boundary conditions this procedure then results in the aimed discretization scheme.

Please cite this article as: M. Ashyraliyev, et al., On the numerical solution of diffusion–reaction equations with singular source terms, J. Comput. Appl. Math. (2007), doi: 10.1016/j.cam.2007.04.017

Correct application of the divergence theorem generally impedes existence and integrability of u_{xx} which does not hold with a Dirac delta function for ϕ.[1] To circumvent this problem we will assume, for the sake of analysis only, that we are solving a modified equation defined by a modified source term associated to $\delta(x-\bar{x})$. More specifically, we will associate $\delta(x-\bar{x})$ with a class of source functions $\phi(x)$ leading to twice continuously differentiable solutions u and which are equivalent with $\delta(x-\bar{x})$ in the sense that

$$\int_{\Omega_i} \phi(x)\,\mathrm{d}x = \int_{\Omega_i} \delta(x-\bar{x})\,\mathrm{d}x, \quad i=1,\ldots,N. \tag{2.5}$$

The divergence theorem is then applicable for these twice continuously differentiable solutions and, furthermore, assuming exact integration or a proper quadrature rule, the ϕ-integrals in (2.4) are computed as if the source is the Dirac delta function. Hence the resulting difference scheme remains unaltered.

In addition to (2.5) we will further assume that any ϕ considered converges uniformly in x to the Dirac delta function with $\mathcal{O}(h)$ in the sense that

$$\int_0^1 G(x,y)(\phi(y)-\delta(y-\bar{x}))\,\mathrm{d}y = \mathcal{O}(h). \tag{2.6}$$

We will show that there exist a function ϕ that satisfies (2.5)–(2.6). Due to (2.2) requirement (2.6) immediately leads to first-order convergence of the exact modified solution u to the sought exact solution. This in turn implies first-order convergence of the numerical solution to the sought solution if we have first-order h-convergence of the numerical solution to the assumed modified solution. Below we will illustrate this line of thinking which is reminiscent of backward error analysis as used in numerical linear algebra or numerical differential equations, see e.g., [2].

To set up the difference scheme let us assume that $\bar{x} \in (x_{j-1/2}, x_{j+1/2})$ for a certain $j = j(h)$ at a distance ch of the cell center x_j, i.e., $\bar{x} = x_j + ch$ with $-\frac{1}{2} < c < \frac{1}{2}$. Then due to (2.5), (2.4) becomes

$$-\frac{u_x(x_{i+1/2})}{h} + \frac{u_x(x_{i-1/2})}{h} = \frac{\delta_{ij}}{h}, \quad i=1,\ldots,N, \tag{2.7}$$

where δ_{ij} is the Kronecker delta symbol. Next, let w_i, $i=1,\ldots,N$, denote the numerical solution for $u(x_i)$ resulting from approximating $u_x(x_{i+1/2})$ in (2.7) by $(u(x_{i+1})-u(x_i))/h$, etc. The Dirichlet boundary values are accounted for by extrapolation to auxiliary values $w_0 = 2u(0) - w_1$, $w_{N+1} = 2u(1) - w_N$ and by insertion of w_0 and w_{N+1} for $i=1$ and N, respectively. If we then assemble the w_i in the grid function $w = (w_1,\ldots,w_N)^{\mathrm{T}}$, we get as numerical scheme the $N \times N$ symmetric linear system[2]

$$-Aw = b, \quad A = \frac{1}{h^2}\begin{pmatrix} -3 & 1 & & & \\ 1 & -2 & 1 & & \\ & \ddots & \ddots & \ddots & \\ & & 1 & -2 & 1 \\ & & & 1 & -3 \end{pmatrix}, \quad b = \frac{1}{h}\begin{pmatrix} 0 \\ . \\ 1 \\ . \\ 0 \end{pmatrix}, \tag{2.8}$$

where b has zero entries except at entry j. The inverse of the difference matrix is bounded uniformly in $h = 1/N$, defining $w = A^{-1}b$ uniquely as the aimed numerical solution.

Let $u_h = (u(x_1),\ldots,u(x_N))^{\mathrm{T}}$ denote the restriction of $u(x)$ to the grid. As discussed above, the numerical solution w can be interpreted as an approximation to u_h for a twice differentiable modified solution u defined by an appropriate source function ϕ satisfying (2.5). Likewise, once constructed, w may also be directly compared to the actually sought solution lying at a maximum norm distance $\mathcal{O}(h)$ to any appropriate modified solution.

[1] Solution (2.3) forms an exception. For this solution the divergence theorem appears to hold over the cell Ω_i containing $\bar{x}$.

[2] The values -3 at the corner entries are due to the fact that we have chosen a cell-centered grid and have Dirichlet boundary values. With a vertex-centered grid (boundary points as cell centers) the common stencil would result with -2 at the corner entries. See Section I.5.3 in [3] for accuracy aspects.

Please cite this article as: M. Ashyraliyev, et al., On the numerical solution of diffusion–reaction equations with singular source terms, J. Comput. Appl. Math. (2007), doi: 10.1016/j.cam.2007.04.017

2.1.1. Error analysis through modified solutions

Associating a uniquely determined numerical solution with different exact modified solutions for the sake of analysis is the central idea of backward error analysis. This line of thinking may enhance insight in the numerical discretization procedure or, as in our case, even justify the discretization procedure. Here we are in the special situation of being able to find the numerical solution and exact modified solutions in closed form. One can easily check that

$$w_i = \begin{cases} x_i(1-x_j), & i = 1, \ldots, j, \\ x_j(1-x_i), & i = j+1, \ldots, N, \end{cases} \tag{2.9}$$

solves (2.8). This numerical solution differs from solution (2.3) only in that $\bar{x}$ is replaced by x_j, revealing a small shift in the peak and an error at all grid points. In terms of $\bar{x}$ and ch, with $-\frac{1}{2} < c < \frac{1}{2}$, we have

$$w_i = \begin{cases} x_i(1-\bar{x}) + cx_i h, & i = 1, \ldots, j, \\ \bar{x}(1-x_i) - c(1-x_i)h, & i = j+1, \ldots, N, \end{cases} \tag{2.10}$$

immediately showing $\mathcal{O}(h)$ maximum norm convergence. For $c = 0$, i.e., with the singular point $\bar{x}$ located in the center of cell Ω_j, the scheme returns the sought solution exactly.

Next consider by way of example the continuous source function

$$\phi(x) = \begin{cases} 0, & 0 \leqslant x \leqslant x_j - h/2, \\ \dfrac{4}{h^2}(x - x_j + h/2), & x_j - h/2 \leqslant x \leqslant x_j, \\ \dfrac{4}{h^2}(x_j - x + h/2), & x_j \leqslant x \leqslant x_j + h/2, \\ 0, & x_j + h/2 \leqslant x \leqslant 1, \end{cases} \tag{2.11}$$

which satisfies (2.5)–(2.6) and results in the twice continuously differentiable modified solution

$$u(x) = \begin{cases} x(1-x_j), & 0 \leqslant x \leqslant x_j - h/2, \\ x(1-x_j) - \dfrac{2}{3h^2}(x - x_j + h/2)^3, & x_j - h/2 \leqslant x \leqslant x_j, \\ x_j(1-x) - \dfrac{2}{3h^2}(x_j - x + h/2)^3, & x_j \leqslant x \leqslant x_j + h/2, \\ x_j(1-x), & x_j + h/2 \leqslant x \leqslant 1. \end{cases} \tag{2.12}$$

On the grid this modified solution is closer to the numerical solution (2.9) than the sought one as it should be. The u_h and w coincide at all grid points except at x_j where the difference is $h/12$. Observe that (2.11) can be interpreted as a regularized form of the singular Dirac delta function as discussed in [8]. Contrary to the approach followed here, in [8] such regularized forms are explicitly used and implemented in the used difference schemes.

2.1.2. Error analysis through the truncation error

Following the common approach of (forward) error analysis we will next examine the convergence of (2.8) to the sought solution u by analyzing the local truncation error σ and global error e defined by

$$\sigma = -Au_h - b, \quad e = u_h - w.$$

There holds $-Ae = \sigma$ so that $\|e\|_\infty \leqslant \|A^{-1}\|_\infty \|\sigma\|_\infty$. Hence if $\|\sigma\|_\infty = \mathcal{O}(h^2)$ we immediately have second-order convergence in view of the uniform boundedness of $\|A^{-1}\|_\infty$. However, for the current solution (2.3) we find

$$\sigma = \left(0, \ldots, 0, \frac{-c}{h}, \frac{c}{h}, 0, \ldots, 0\right)^{\mathrm{T}} \tag{2.13}$$

Please cite this article as: M. Ashyraliyev, et al., On the numerical solution of diffusion–reaction equations with singular source terms, J. Comput. Appl. Math. (2007), doi: 10.1016/j.cam.2007.04.017

with nonzero entries for cells j and $j+1$, respectively. Here it is assumed that $\bar{x}$ lies at the right of x_j so that $0 \leqslant c < \frac{1}{2}$. With $\bar{x}$ at the left the nonzero entries shift to cells $j-1$, j. For $c = 0$, i.e., with the singular point located at the center of cell Ω_j, a zero truncation error results and hence in this special case the scheme returns the exact solution (2.3). In all other cases $\|\sigma\|_\infty = \mathcal{O}(h^{-1})$ so that convergence cannot be concluded when the standard argument sketched above is followed.

Through a more subtle local truncation error analysis the correct maximum norm $\mathcal{O}(h)$ convergence can be proven, however, gaining two powers of h. A similar situation generally occurs with Dirichlet boundary conditions due to the cell-centered location of x_1 and x_N half a distance h away from the boundary. For a general smooth solution we then would have $\sigma_1 = \mathcal{O}(1)$, $\sigma_N = \mathcal{O}(1)$. In [3, Section I.5.3], it is shown that we then still can expect second-order convergence (with a sufficiently smooth source) due to a favorable local error cancellation and we adopt here the method of proof of [3] to show first-order convergence with σ given by (2.13) using the following ansatz: the local truncation error can be decomposed as $\sigma = -Ar + \xi$ such that the grid functions r, ξ are componentwise $\mathcal{O}(h)$. This would immediately prove first-order convergence since the global error then satisfies $e = r - A^{-1}\xi$. The ansatz is verified as follows. Put $\xi = 0$ and $r = h\alpha$. We then have to verify that such a grid function α exists and satisfies $\alpha = \mathcal{O}(1)$ componentwise. The result is

$$\alpha_i = \begin{cases} \dfrac{1-2i}{2N}c, & i = 1, \ldots, j, \\ \dfrac{2N-2i+1}{2N}c, & i = j+1, \ldots, N, \end{cases} \tag{2.14}$$

which completes the proof. Observe that since $\xi = 0$ we have $e = h\alpha$ connecting this expression with (2.9) through $w = u_h - h\alpha$.

Example 2.1. As a second illustration of the $\mathcal{O}(h)$ convergence of the cell-centered scheme we consider a slight extension of the 1D test model (2.1), viz.,

$$-u_{xx} + u = \delta(x - \bar{x}), \quad 0 < x < 1, \tag{2.15}$$

again with homogeneous Dirichlet boundary conditions. This problem does have as solution

$$u(x) = \begin{cases} \dfrac{\sinh(1-\bar{x})\sinh(x)}{\sinh(1)}, & 0 \leqslant x \leqslant \bar{x}, \\ \dfrac{\sinh(1-x)\sinh(\bar{x})}{\sinh(1)}, & \bar{x} \leqslant x \leqslant 1. \end{cases}$$

Fig. 1 shows u (left plot, solid line) for $\bar{x} = \frac{1}{3}$ along with the cell-centered solution for $h = \frac{1}{20}$ (o-marks). The plot at the right nicely reveals the anticipated first-order convergence ($\|u_h - w\|_\infty$ versus h in log–log scale).

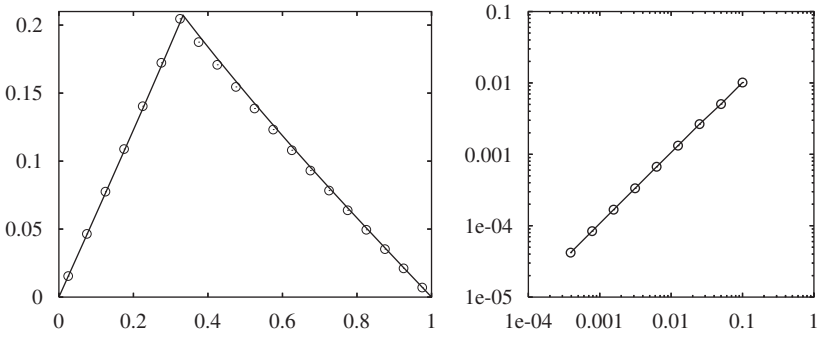

Fig. 1. Numerical illustration for problem (2.15) with $\bar{x} = \frac{1}{3}$ on the uniform grid.

Please cite this article as: M. Ashyraliyev, et al., On the numerical solution of diffusion–reaction equations with singular source terms, J. Comput. Appl. Math. (2007), doi: 10.1016/j.cam.2007.04.017

2.2. The 2D boundary value problem

An interesting 2D test model used in [8] is the Poisson equation

$$-\Delta u = \delta(\Gamma, x, y). \tag{2.16}$$

Here the source denotes the Dirac delta function along a curve Γ defined by

$$\int_{\mathbb{R}^2} \delta(\Gamma, x, y)\,\mathrm{d}x\,\mathrm{d}y = \int_{\Gamma} \mathrm{d}\gamma, \tag{2.17}$$

with co-ordinate γ on Γ.

As in the 1D test model case, the solution u is continuous but not continuously differentiable across Γ so that the divergence theorem cannot be correctly applied. However, by arguing with assumptions similar to (2.5), (2.6), the divergence theorem is correctly applied for twice differentiable modified solutions.

Assuming (2.16) on a square, and using a uniform $N \times N$ grid the 2D counterpart of (2.8) reads

$$-(A \otimes I_N + I_N \otimes A)w = b, \tag{2.18}$$

where I_N is the identity matrix of size N and $\otimes$ is the direct matrix (Kronecker) product. The entries b_k of the vector $b \in \mathbb{R}^{N\times N}$ are associated to grid cells Ω_{ij} with values emanating from the boundary conditions and the source $\delta(\Gamma, x, y)$. Considering the source contribution, let $\Gamma_{ij} = \Gamma \cap \Omega_{ij}$ and $|\Gamma_{ij}|$ the length of Γ_{ij}. Then, assuming exact integration of the integral along Γ, from (2.17) and the finite volume approach follows that either

$$b_k = |\Gamma_{ij}|/h^2 \tag{2.19}$$

or $b_k = 0$ (considering only the source term contribution). Because upon intersection $|\Gamma_{ij}|$ is proportional to h, assuming h sufficiently small, b_k is then proportional to $1/h$ or equal to zero, similar as in the 1D case.

For the circle $\Gamma = \{(x, y) : (x - x_c)^2 + (y - y_c)^2 = r^2\}$ problem (2.16) has the radial symmetric solution [8]

$$u(x, y) = \begin{cases} u_\Gamma, & (x - x_c)^2 + (y - y_c)^2 \leqslant r^2, \\ u_\Gamma - r\,\log\left(\dfrac{\sqrt{(x - x_c)^2 + (y - y_c)^2}}{r}\right), & (x - x_c)^2 + (y - y_c)^2 \geqslant r^2, \end{cases} \tag{2.20}$$

where u_Γ is a given constant value on Γ. For $u_\Gamma = 1$, $r = \frac{1}{4}$ and $(x_c, y_c) = (\frac{1}{2}, \frac{1}{2})$ we have applied (2.18) on the unit square $0 < x, y < 1$ with Dirichlet boundary values prescribed from (2.20). Like in the 1D case this results in order reduction from two to one. Fig. 2 shows the corresponding u and nicely illustrates the first-order convergence of (2.18). The right figure plots $\|u_h - w\|_\infty$ versus h in log–log scale. We have used exact integration along Γ (for the circle this is straightforward).

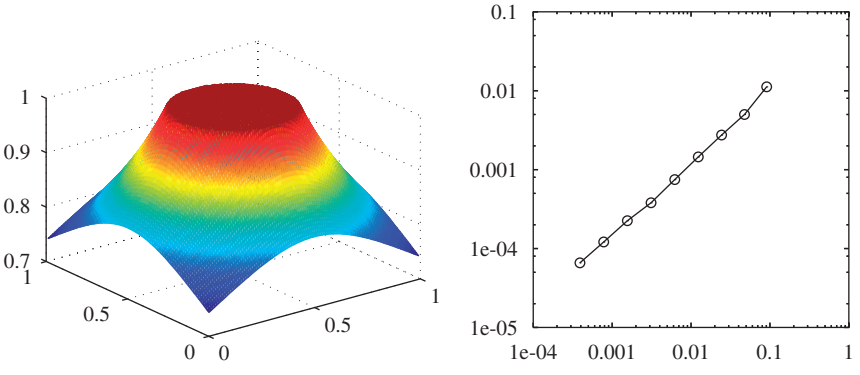

Fig. 2. Numerical illustration for problem (2.16)–(2.20) on the uniform grid.

Please cite this article as: M. Ashyraliyev, et al., On the numerical solution of diffusion–reaction equations with singular source terms, J. Comput. Appl. Math. (2007), doi: 10.1016/j.cam.2007.04.017

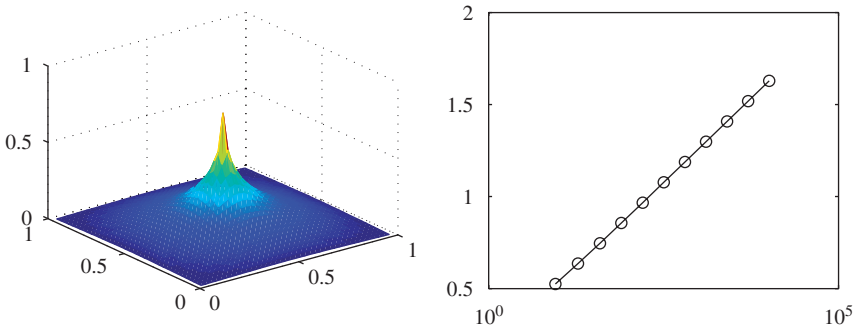

Fig. 3. Numerical illustration for the ill-posed 2D problem from Remark 2.2.

Remark 2.2. No finite solution exists when using the 2D Dirac delta function at a point. To see this, consider $-\Delta u = \delta(x-\frac{1}{2}, y-\frac{1}{2})$ on the unit square with homogeneous Dirichlet boundary values. Introduce the uniform vertex-centered (cell centers at the boundary) $N \times N$ grid with grid size $h = 1/(N+1)$ and assume N odd. Applying as above the finite volume approach over all internal $h \times h$ grid cells then leads to a linear system $\mathscr{A}w = b$ of type (2.18) where A is defined as in (2.8), except that at the corner points -3 is replaced by -2 (the standard stencil for homogeneous Dirichlet boundary values). Further, vector b has all its components equal to zero, except at entry $k = (N^2+1)/2$ associated to the center point $(\frac{1}{2}, \frac{1}{2})$. Here $b_k = 1/h^2$ due to

$$\int_{\mathbb{R}^2} \delta(x-1/2, y-1/2) = 1.$$

Since $\mathscr{A}$ is symmetric, its inverse satisfies $\mathscr{A}^{-1} = XD^{-1}X^{\mathrm{T}}$ with eigenvector matrix X and eigenvalue matrix D. Consequently, $w_k = (r_k \cdot D^{-1} r_k^{\mathrm{T}})/h^2$ where r_k is the kth row of X. Using the known expressions for the eigenvectors and eigenvalues [3, Section III.6.2], we then find the expression

$$w_k = \sum_{\text{odd } i,j=1}^{N} 1/\mu_{ij}, \quad \mu_{ij} = h^{-2}\left(\sin^2\left(\frac{\pi i h}{2}\right) + \sin^2\left(\frac{\pi j h}{2}\right)\right), \quad h = \frac{1}{N+1}$$

for the numerical solution at the center point $(\frac{1}{2}, \frac{1}{2})$. Fig. 3 plots the numerical solution on the 39×39 grid (left plot) and w_k as a function of increasing N-values (right plot; $N = 10 \cdot 2^l - 1$, $l = 0, 1, \ldots, 10$). Even on fine grids w_k is of moderate size, but it is obvious that $w_k \to \infty$ for $N \to \infty$. Since the w_k-sequence is defined by a convergent scheme we conclude that no finite solution exists. It can be shown analytically [6,7] that $w_k \sim (2\pi)^{-1} \log(N)$ for $N \to \infty$ confirming the growth shown in the figure.

Remark 2.3. On any fixed grid no matter how fine, the strength of the Γ-source will vanish upon shrinking Γ due to (2.17). The strength is kept by scaling (dividing) the source by $|\Gamma|$, the length of Γ. Such scaling will replace (2.19) by $b_k = (|\Gamma_{i,j}|/|\Gamma|)/h^2$ and hence if Γ lies in one or only a few grid cells we have, respectively, $b_k = 1/h^2$ as if we have a point source, or $b_k \approx 1/h^2$. This situation will lead to irregular peak behavior upon grid refinement when initially Γ lies in one cell. First, as long as Γ lies in this same one cell, the peak height will increase, cf. Remark 2.2. Then, when Γ becomes distributed over a few cells, the height will decrease till it eventually settles down when there are enough intersections. Needless to say that this type of irregular behavior may also occur with unscaled sources, but then with a factor h smaller. Small-scaled sources simply require finer grids to achieve the same level of absolute errors.

2.3. Linear time-dependent problems

The step from boundary value problems to time-dependent problems with singular source terms is not large. Consider in a spatial domain $\Omega \in \mathbb{R}^d$ the general, constant coefficient, second order, linear test model

$$u_t = Lu + \phi(\underline{x}), \quad t > 0, \quad \underline{x} \in \Omega, \tag{2.21}$$

Please cite this article as: M. Ashyraliyev, et al., On the numerical solution of diffusion–reaction equations with singular source terms, J. Comput. Appl. Math. (2007), doi: 10.1016/j.cam.2007.04.017

provided with an initial function $u(\underline{x}, 0)$ at time zero, appropriate boundary conditions for $t > 0$, and a singular source term ϕ. The spatial discretization and source treatment through the finite volume approach goes essentially the same as in the boundary value case.

For any volume or grid box $V \in \mathbb{R}^d$ it starts from the integral form

$$\frac{\partial}{\partial t}\frac{\int_V u \,\mathrm{d}\underline{x}}{\int_V \mathrm{d}\underline{x}} = \frac{\int_V Lu \,\mathrm{d}\underline{x}}{\int_V \mathrm{d}\underline{x}} + \frac{\int_V \phi(\underline{x}) \,\mathrm{d}\underline{x}}{\int_V \mathrm{d}\underline{x}}.$$

For the u_t-integral term we will suppose the midpoint quadrature rule approximating the left-hand side by a value $w'_V(t)$ say where $'$ denotes $\mathrm{d}/\mathrm{d}t$. As in the boundary value case we will interpret ϕ to be a source function giving rise to a twice continuously differentiable solution $u(\underline{x}, t)$ so that we may apply the divergence theorem for Lu. This ϕ is then supposed to satisfy a counterpart of (2.5) for the singular source under consideration, so that we end up with a semi-discrete central difference scheme identical to that for the singular source.

The scheme takes the generic form of a linear, constant coefficient ODE system

$$w'(t) = Aw(t) + b, \quad t > 0, \quad w(0) = w_0, \tag{2.22}$$

the solution of which can be expressed as

$$w(t) = \mathrm{e}^{At} w(0) + (\mathrm{e}^{At} - I)\, A^{-1} b. \tag{2.23}$$

If the exponential operator satisfies $\exp(At) \to 0$ for $t \to \infty$, this solution results in the steady state $w = -A^{-1}b$ for $t \to \infty$. The spatial error analysis for finite t is almost identical to the analysis for the stationary case. The local truncation error σ and global error e are now defined by

$$\sigma(t) = u'_h(t) - Au_h(t) - b, \quad e(t) = u_h(t) - w(t)$$

and come together in the global error equation

$$e'(t) = Ae(t) + \sigma(t), \quad t > 0, \quad e(0) = u_h(0) - w(0).$$

Assuming bounds on the exponential matrix, $e(t)$ then can be expressed in bounds on $\sigma(t)$. Hereby one should use a refined error analysis similar as shown above to cater for local order reduction coming from a singular source. Such a refined error analysis can be found in [3, Section I.5.3], for a similar reduction coming from the boundary. These results carry over to reduction caused by singular sources.

The final assumption is that a counterpart of (2.6) is satisfied so that the modified solution lies at a maximum norm distance $\mathcal{O}(h)$ of the solution u generated by the singular source. First-order maximum norm convergence of $w(t)$ for the modified solution then results automatically in first-order maximum norm convergence to u. What then remains is to turn the continuous time solution $w(t)$ in a fully discrete solution by numerical time integration (method of lines). There exists a great deal of choices of integrators, depending on issues like stiffness, stability, consistency and efficiency [3]. In the next section we will pick one in a numerical illustration for a time-dependent problem with a nonlinear source.

2.4. Nonlinear time-dependent problems

We will next consider a nonlinear extension of the linear test models discussed in the previous section. Our aim is to include singular nonlinear reaction terms, singular in the sense that the chemical reactions are confined to a lower dimensional surface Γ in the space domain $\Omega \subset \mathbb{R}^d$, similar as before. The nonlinear test model has the time-dependent form

$$u_t = Lu + \delta(\Gamma, \underline{x})\, R(\underline{x}, t, u), \quad \underline{x} \in \Omega, \quad t > 0. \tag{2.24}$$

The definition of L is here of secondary importance. For simplicity of presentation we assume that Lu is the linear elliptic form $Lu = \nabla \cdot (D\nabla u)$ with $D \in \mathbb{R}^{d\times d}$ diagonal and dependent on $\underline{x}$ only. The source term is supposed to satisfy the Dirac delta function relation [8]

$$\int_{\mathbb{R}^d} \delta(\Gamma, \underline{x}) R(\underline{x}, t, u) \,\mathrm{d}\underline{x} = \int_\Gamma R(\underline{x}(\gamma), t, u) \,\mathrm{d}\gamma \tag{2.25}$$

Please cite this article as: M. Ashyraliyev, et al., On the numerical solution of diffusion–reaction equations with singular source terms, J. Comput. Appl. Math. (2007), doi: 10.1016/j.cam.2007.04.017

with co-ordinate γ on Γ. The dependent variable $u(\underline{x}, t)$ is supposed to represent s concentrations, hence u is a vector $u=(u_1, \ldots, u_s)$ and accordingly the nonlinear vector function $R(\underline{x}, t, u)$ has also s components. Providing (2.24) with appropriate initial and boundary conditions yields the initial-boundary value problem we wish to solve.

The focus of our investigation lies in the singular source term treatment and for this purpose we take $d=2$ with $\Omega=(-1, 1)^2$ and assume for space discretization the finite volume approach with centered finite differences on a uniform $N \times N$-grid with grid size $h=2/N$, similar to the linear case presented in Section 2.2. This space discretization leads to the following nonlinear counterpart of system (2.22),

$$w'(t) = Aw(t) + b\,(t, w(t))\,, \quad t>0, \quad w(0)=w_0. \tag{2.26}$$

With a smooth source term defined on the whole of Ω we would have second-order consistency. However, the singular source term will lead to first-order consistency and what remains to show is how this term enters the nonlinear vector function $b(t, w)$. Consider a grid cell Ω_{ij} and recall the derivation in Section 2.2. If $\Gamma \cap \Omega_{ij} = \emptyset$, the corresponding contributions to b are zero. If $\Gamma \cap \Omega_{ij} \neq \emptyset$, these contributions are unequal zero and are obtained from the first-order approximation

$$|\Gamma_{ij}|\, R(\underline{x}_{ij}, t, u(\underline{x}_{ij}, t)) \approx \int_{\Gamma_{ij}} R(\underline{x}(\gamma), t, u)\, \mathrm{d}\gamma.$$

Associating the index pair (i, j) with an index k for b, we thus get

$$b_k = |\Gamma_{ij}|\, R(\underline{x}_k, t, w_k)/h^2. \tag{2.27}$$

The computation of b thus goes essentially the same as in the linear case with regard to the singular source term treatment, the only difference being that b_k is nonlinear in the cell-center value w_k. This might complicate the numerical integration in time, but should form otherwise no obstacle for obtaining a fully discrete numerical solution.

Remark 2.4. Two invariants for u are positivity (componentwise non-negativity) and mass conservation. We distinguish molecular and spatial mass conservation. The first emanates from the mass action law of chemical kinetics [3] and amounts to the existence of constant, nonnegative weight vectors $v=(v_1, \ldots, v_s)^{\mathrm{T}}$, such that for any solution of the ODE system $u'=R(\underline{x}, t, u)$ the inner product $v^{\mathrm{T}}u(\underline{x}, t)$ is constant in time (the molecular mass defined by v). Trivially, this holds iff $v^{\mathrm{T}}R(\underline{x}, t, w)=0$ for any $w \in \mathbb{R}^s$. The spatial conservation depends on the boundary conditions, as usual. Combining these two properties will reveal conservation of the total mass

$$M(t) = \int_{\Omega} v^{\mathrm{T}} u(\underline{x}, t)\, \mathrm{d}\underline{x}$$

associated to a given v. To see this, we compute

$$M'(t) = \int_{\Omega} v^{\mathrm{T}} (\nabla \cdot (D\nabla u) + \delta(\Gamma, \underline{x})\, R(\underline{x}, t, u))\, \mathrm{d}\underline{x},$$

and due to (2.25), molecular mass conservation, and the divergence theorem, we have

$$M'(t) = \int_{\Omega} v^{\mathrm{T}}\, (\nabla \cdot (D\nabla u))\, \mathrm{d}\underline{x} = \sum_{i=1}^{s} \int_{\delta\Omega} (D\nabla u_i) \cdot \mathbf{n}\, \mathrm{d}\underline{x}$$

and get as usual that the fluxes over the boundary determine conservation of the total mass.

Since we use the finite volume approach for spatial discretization this argument applies to any grid box and the standard result will then be that for the semi-discrete solution $w(t)$, $M(t)$ will be approximated over the space grid (to at least first-order in space) by a linear functional $M_h(t)=Q^{\mathrm{T}}w(t)$ which mimics the time evolution of $M(t)$. In particular, $M_h(t)$ will be constant in time if this holds for $M(t)$ and any Runge–Kutta or linear multistep method will mimic this in the time integration because these methods conserve linear invariants, see [2, Section IV.1.5].

Positivity of (2.24) under discretization depends on the spatial discretization and the time integration. The central scheme we favor here for approximating (2.24) by (2.26) is positive [3, Section I.7]. To guarantee unconditional positivity in time, that is, for any step size $\tau>0$, we are bound to the first-order implicit Euler method [3]. We prefer

Please cite this article as: M. Ashyraliyev, et al., On the numerical solution of diffusion–reaction equations with singular source terms, J. Comput. Appl. Math. (2007), doi: 10.1016/j.cam.2007.04.017

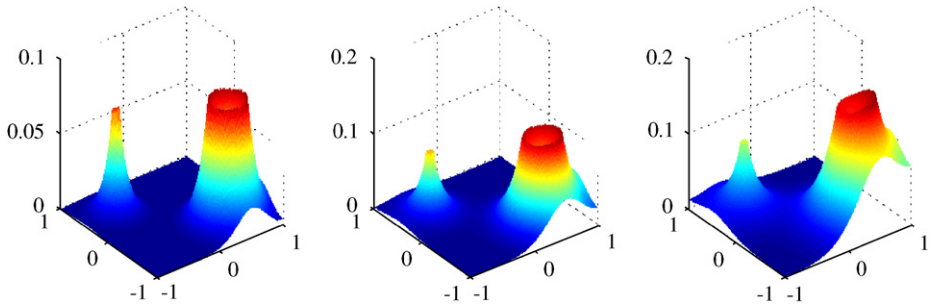

Fig. 4. Numerical illustration for the problem from Example 2.5.

however to sacrifice this guarantee in favor of more time accuracy and will instead use a second-order IMEX version of the second-order BDF method.

Example 2.5. We will solve (2.24)–(2.27) for the reversible reaction $2[u_2] \overset{k}{\rightleftharpoons} [u_1] + [u_2]$, giving

$$R(u) = \begin{cases} -ku_1u_2 + ku_2^2, \\ -ku_2^2 + ku_1u_2. \end{cases}$$

The corresponding ODE system $u' = R(u)$ has the exact solution

$$u_1(t) = \frac{s_0}{2}\frac{1 - \alpha + 2\alpha\,\mathrm{e}^{-s_0kt}}{1 - \alpha + \alpha\,\mathrm{e}^{-s_0kt}}, \quad u_2(t) = s_0 - u_1(t),$$

where $\alpha = (2u_1(0) - s_0)/s_0$ and $s_0 = u_1(t) + u_2(t)$ which is constant in time (linear invariant). For $t \to \infty$ the ODE solution (u_1, u_2) approaches the steady state $(s_0/2, s_0/2)$ exponentially fast. Here we take $k = 1$ and a finite time interval since we are interested in transient behavior. For the PDE system we choose for the diffusion part the Laplace operator, $u_1(x, y, 0) = 0$ and $u_2(x, y, 0) = s_0 = 1$ for initial functions, and homogeneous Neumann (no flux) for boundary conditions. Due to the no-flux condition, $u_1(x, y, t) + u_2(x, y, t) \equiv s_0$. For Γ we define two circles $(x - x_0)^2 + (y - y_0)^2 = r^2$ with, respectively, the center points $(.5, -.5)$, $(-.5, .5)$ and radii .05, .25. As in Section 2.2 the $|\Gamma_{ij}|$ are computed exactly.

For reasonable grid sizes h the parabolic linear part Aw in (2.26) will readily be stiff. The reaction constant $k = 1$ does not introduce stiffness for the nonlinear term $b(t, w)$, but due to its singular nature this term has entries proportional to $|\Gamma_{ij}|/h^2 \sim 1/h$ which causes it to be mildly stiff. For time integration we can therefore use the following implicit–explicit (IMEX) version of the BDF2 scheme [3, Section IV.4],

$$w_{n+1} = \tfrac{4}{3}w_n - \tfrac{1}{3}w_{n-1} + \tfrac{2}{3}\tau A w_{n+1} + \tfrac{2}{3}\tau(2b(t_n, w_n) - b(t_{n-1}, w_{n-1})). \tag{2.28}$$

This IMEX scheme treats the linear part implicitly and the nonlinear part explicitly and thus avoids nonlinear equation solutions. It does retain the second-order of consistency of BDF2 and if we take τ proportional to h it can deal with the modest stiffness introduced by the singular source. For the first integration step, the similar IMEX form of implicit Euler [3] is used to provide the additional starting value w_1.

For $h = \frac{2}{199}$ and $\tau = \frac{1}{200}$ Fig. 4 shows the computed u_1-field at $t = 0.025$ (left), 0.05 (middle), 0.1 (right). Recall that at time $t = 0$ the u_1-field is zero and note the difference in vertical scaling to see that on the current time interval both sources survive diffusion. The growth along the larger circle is larger due to the greater source strength.

2.5. Discussion

In this section we have studied the finite volume discretization on a uniform grid for a number of linear and nonlinear test problems. This spatial discretization, being second-order convergent in the maximum norm for smooth problems, does suffer here from order reduction to first-order maximum norm convergence. Its advantage is that it is straightforward and that it leads to symmetric, well-structured matrices which makes it easy to solve a linear system. However, with

Please cite this article as: M. Ashyraliyev, et al., On the numerical solution of diffusion–reaction equations with singular source terms, J. Comput. Appl. Math. (2007), doi: 10.1016/j.cam.2007.04.017

first-order convergence, only modest accuracy levels can be achieved and the question arises whether second order can be obtained in a feasible way through local grid refinement. We will address this question in the next section.

3. The finite volume approach on locally refined grids

In this section we will study the finite volume discretization on special locally refined grids for the linear 1D and 2D test models from Section 2. Our main aim is to obtain a numerical scheme which converges with second order in the maximum norm.

3.1. The 1D boundary value problem

We start again with the boundary value problem for the 1D equation

$$-u_{xx} = \delta(x - \bar{x}), \quad 0 < x < 1, \quad \bar{x} \in (0, 1), \tag{3.1}$$

provided with the homogeneous Dirichlet conditions $u(0) = 0$, $u(1) = 0$. The exact solution of this problem is given by (2.3). In this section we will consider grid refinement near $\bar{x}$.

Let $h = 1/N$ where N is the number of uniform grid cells $\Omega_i = [(i-1)h, ih]$ for $i = 1, \ldots, N$ covering $[0, 1]$. Let $x_i = (i - 1/2)h$ denote the cell center of Ω_i. The easiest way to refine the grid would be to divide grid cell Ω_j containing $\bar{x}$, now called a coarse grid cell, into two small grid cells in such a way that $\bar{x}$ is the center of one of them. It is not difficult to show that the numerical scheme obtained through finite volume discretization on this locally refined grid returns the sought solution exactly. However, this idea to refine the grid is not extendable to the 2D case. So we introduce a different way to refine the grid.

Let $D_i = [(i-1)h, ih] = \Omega_i$ for $i = 1, \ldots, j-1$ and $D_i = [(i-3)h, (i-2)h] = \Omega_{i-2}$ for $i = j+3, \ldots, N+2$. To define the new grid cells D_j, D_{j+1} and D_{j+2}, we divide the grid cell Ω_j into N small uniform grid cells $\Omega_j^1, \ldots, \Omega_j^N$ with grid sizes h^2. Assume that $\bar{x} \in \Omega_j^k$. Then we take

$$D_j = \Omega_j^1 \cup \cdots \cup \Omega_j^{k-1}, \quad D_{j+1} = \Omega_j^k, \quad D_{j+2} = \Omega_j^{k+1} \cup \cdots \cup \Omega_j^N.$$

So, grid cells D_i for $i = 1, \ldots, j-1, j+3, \ldots, N+2$ have grid size h, grid cell D_j has grid size $h_l = (k-1)h^2$, grid cell D_{j+1} has grid size h^2 and grid cell D_{j+2} has grid size $h_r = (N-k)h^2$. We will call grid cells D_i for $i = 1, \ldots, j-2$ and $i = j+4, \ldots, N+2$ regular cells and D_i for $i = j-1, \ldots, j+3$ irregular cells. Let y_i denote the cell center of D_i for $i = 1, \ldots, N+2$. Let v_i for $i = 1, \ldots, N+2$ denote the finite volume approximation of the exact solution of problem (3.1) on the refined grid.

The finite volume discretization of (3.1) for regular cells which are at least one cell away from the boundaries gives us

$$-\frac{1}{h^2}(v_{i-1} - 2v_i + v_{i+1}) = 0, \quad i = 2, \ldots, j-2, \quad i = j+4, \ldots, N+1. \tag{3.2}$$

For the boundary grid cells, having homogeneous Dirichlet boundary conditions, we get

$$-\frac{1}{h^2}(v_2 - 3v_1) = 0, \quad -\frac{1}{h^2}(v_{N+1} - 3v_{N+2}) = 0. \tag{3.3}$$

Next we derive the finite volume discretization for the irregular cells shown in Fig. 5.

Integrating (3.1) over D_{j-1}, dividing by the cell volume h and applying the divergence (Gauss) theorem gives

$$-\frac{u_x(y_{j-1/2})}{h} + \frac{u_x(y_{j-3/2})}{h} = 0.$$

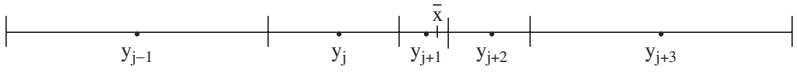

Fig. 5. The irregular cells $D_{j-1}, \ldots, D_{j+3}$ with their cell centers.

Please cite this article as: M. Ashyraliyev, et al., On the numerical solution of diffusion–reaction equations with singular source terms, J. Comput. Appl. Math. (2007), doi: 10.1016/j.cam.2007.04.017

By approximating $u_x(y_{j-3/2})$ by $(v_{j-1}-v_{j-2})/h$ and $u_x(y_{j-1/2})$ by $(2/(h+h_l))(v_j-v_{j-1})$, we get

$$-\frac{1}{h^2}v_{j-2}+\left(\frac{1}{h^2}+\frac{2}{h(h+h_l)}\right)v_{j-1}-\frac{2}{h(h+h_l)}v_j=0,$$

or, equivalently,

$$-\frac{1}{h^2}\left[v_{j-2}-\left(1+\frac{2h}{h+h_l}\right)v_{j-1}+\frac{2h}{h+h_l}v_j\right]=0. \tag{3.4}$$

Despite the fact that the approximation for $u_x(y_{j-1/2})$ is first order as it is non-centered, we will show later that the obtained numerical scheme does converge with second order in the maximum norm.

Working along the remaining irregular cells D_j, D_{j+1}, D_{j+2}, D_{j+3} we find the discretizations

$$-\frac{1}{h^2}\left[\frac{2h^2}{h_l(h+h_l)}v_{j-1}-\left(\frac{2h^2}{h_l(h+h_l)}+\frac{2h^2}{h_l(h^2+h_l)}\right)v_j+\frac{2h^2}{h_l(h^2+h_l)}v_{j+1}\right]=0, \tag{3.5}$$

$$-\frac{1}{h^2}\left[\frac{2}{h^2+h_l}v_j-\left(\frac{2}{h^2+h_l}+\frac{2}{h^2+h_r}\right)v_{j+1}+\frac{2}{h^2+h_r}v_{j+2}\right]=\frac{1}{h^2}, \tag{3.6}$$

$$-\frac{1}{h^2}\left[\frac{2h^2}{h_r(h^2+h_r)}v_{j+1}-\left(\frac{2h^2}{h_r(h^2+h_r)}+\frac{2h^2}{h_r(h+h_r)}\right)v_{j+2}+\frac{2h^2}{h_r(h+h_r)}v_{j+3}\right]=0, \tag{3.7}$$

$$-\frac{1}{h^2}\left[\frac{2h}{h+h_r}v_{j+2}-\left(1+\frac{2h}{h+h_r}\right)v_{j+3}+v_{j+4}\right]=0. \tag{3.8}$$

Combining (3.2)–(3.8), we obtain a $(N+2)\times(N+2)$ tridiagonal linear system

$$-\tilde{A}v=\tilde{b},\quad \tilde{b}=\frac{1}{h^2}\begin{pmatrix}0\\ .\\ 1\\ .\\ 0\end{pmatrix}, \tag{3.9}$$

where $\tilde{b}$ has zero entries except at entry $j+1$ and $\tilde{A}$ has the same form as A in (2.8) except the entries at rows $j-1,\ldots,j+3$. An elementary calculation then gives the following solution:

$$v_i=\begin{cases}y_i(1-y_{j+1}), & i=1,\ldots,j,\\ y_{j+1}(1-y_i), & i=j+1,\ldots,N+2.\end{cases} \tag{3.10}$$

Since $\bar{x}\in D_{j+1}$, we can write $\bar{x}=y_{j+1}+\gamma h^2$ with $-\frac{1}{2}<\gamma<\frac{1}{2}$, so that (3.10) can be written as

$$v_i=\begin{cases}y_i(1-\bar{x})+\gamma y_i h^2, & i=1,\ldots,j,\\ \bar{x}(1-y_i)-\gamma(1-y_i)h^2, & i=j+1,\ldots,N+2,\end{cases} \tag{3.11}$$

immediately showing $\mathcal{O}(h^2)$ maximum norm convergence by comparison with (2.3), at the expense of only two additional grid cells.

3.1.1. Error analysis based on the truncation error

Following the common approach of error analysis as in Section 2.1 we will next examine the convergence of (3.9) to the sought solution u by analyzing the local truncation error σ and global error e defined by

$$\sigma=-\tilde{A}u_h-\tilde{b},\quad e=u_h-v,$$

Please cite this article as: M. Ashyraliyev, et al., On the numerical solution of diffusion–reaction equations with singular source terms, J. Comput. Appl. Math. (2007), doi: 10.1016/j.cam.2007.04.017

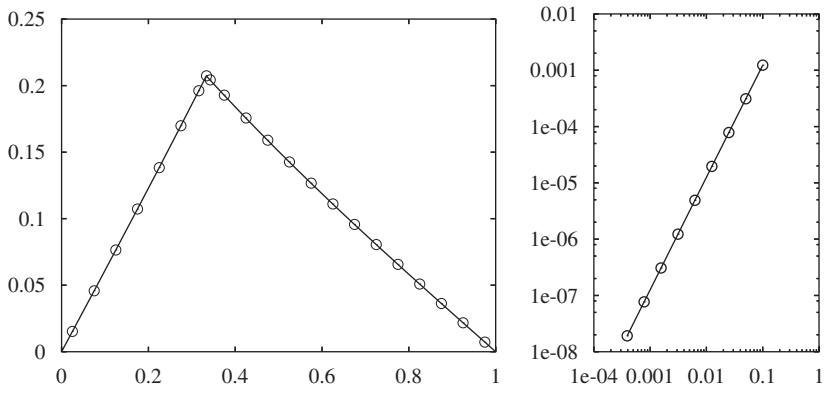

Fig. 6. Numerical illustration for problem (2.15) with $\bar{x} = \frac{1}{3}$ on the locally refined grid.

where u_h denotes u restricted to the refined grid. Note that matrix $\tilde{A}$ is tridiagonal nonsymmetric. It can be shown that there exist a symmetric tridiagonal matrix B and a diagonal matrix D such that $B = D\tilde{A}D^{-1}$, see [4, p. 51]. From the uniform boundedness of $\|B^{-1}\|_\infty$, $\|D^{-1}\|_\infty$ and $\|D\|_\infty$ the uniform boundedness of $\|\tilde{A}^{-1}\|_\infty$ can be concluded.

There holds $-\tilde{A}e = \sigma$ so that $\|e\|_\infty \leqslant \|\tilde{A}^{-1}\|_\infty \|\sigma\|_\infty$. For the current solution (2.3) we find

$$\sigma = \left(0, \ldots, 0, \frac{-2\gamma}{h_r + h^2}, \frac{2\gamma h^2}{h_r(h_r + h^2)}, 0, \ldots, 0\right)^{\mathrm{T}} \tag{3.12}$$

with nonzero entries for cells $j+1$ and $j+2$, respectively. Here it is assumed that $\bar{x}$ lies at the right of y_{j+1} so that $0 \leqslant \gamma < 1/2$. So, in the case where $\gamma \neq 0$ we have $\|\sigma\|_\infty = \mathcal{O}(h^{-2})$ and convergence cannot be concluded.

Through the more subtle local truncation error analysis used in Section 2.1 the correct maximum norm $\mathcal{O}(h^2)$ convergence can be proven. We pose the ansatz that the local truncation error can be decomposed as $\sigma = -\tilde{A}r$ with $r = h^2\alpha$. We then have to verify that such a grid function α exists and satisfies $\alpha = \mathcal{O}(1)$ componentwise. The result is

$$\alpha_i = \begin{cases} -\gamma y_i, & i = 1, \ldots, j+1, \\ \gamma(1 - y_i), & i = j+2, \ldots, N+2, \end{cases} \tag{3.13}$$

which completes the proof. Observe that we have $e = h^2\alpha$ connecting this expression with (3.10) through $v = u_h - h^2\alpha$.

Example 3.1. As an illustration of the $\mathcal{O}(h^2)$ convergence of the locally refined approach we again consider problem (2.15) with homogeneous Dirichlet boundary conditions. Fig. 6 shows u (left plot, solid line) for $\bar{x} = \frac{1}{3}$ along with the numerical solution on the locally refined grid for $h = \frac{1}{20}$ (o-marks). The plot at the right nicely reveals the anticipated second-order convergence ($\|u_h - v\|_\infty$ versus h in log–log scale).

3.2. The 2D boundary value problem

We consider the boundary value problem (2.16)–(2.17) on the unit square $0 \leqslant x, y \leqslant 1$ with Dirichlet boundary conditions prescribed from (2.20). In this section we will examine a number of different approaches for grid refinement near the curve Γ, similar as in Section 3.1, so as to obtain a second-order discretization scheme. We start with a uniform $N \times N$ grid and from now on call the grid cells $\Omega_{i,j}$, $i = 1, \ldots, N$, $j = 1, \ldots, N$ coarse grid cells.

3.2.1. First approach

The easiest way to refine the grid is to divide every coarse grid cell $\Omega_{I,J}$ intersected by Γ uniformly into N^2 small grid cells with grid size h^2. Let us denote such cells by $\Omega_{I,J}^{m,k}$, $m = 1, \ldots, N$, $k = 1, \ldots, N$, where I, m are column indices and J, k are row indices. For simplicity we take N to be odd. We will now discuss the finite volume discretization for one particular grid cell $\Omega_{i,j}$.

Please cite this article as: M. Ashyraliyev, et al., On the numerical solution of diffusion–reaction equations with singular source terms, J. Comput. Appl. Math. (2007), doi: 10.1016/j.cam.2007.04.017

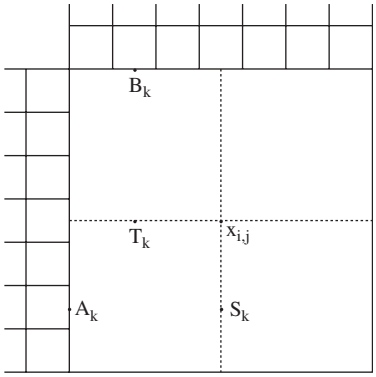

Fig. 7. Grid cell $\Omega_{i,j}$ with its auxiliary points (first approach).

First assume that $\Omega_{i,j}$ is at least one cell away from the boundary. Also assume that Γ intersects the neighboring grid cells $\Omega_{i-1,j}$ and $\Omega_{i,j+1}$ and that it does not intersect $\Omega_{i,j}$, $\Omega_{i+1,j}$, $\Omega_{i,j-1}$. So, $\Omega_{i,j}$ has as neighboring cells $\Omega_{i+1,j}$, $\Omega_{i,j-1}$, $\Omega_{i-1,j}^{N,k}$, $\Omega_{i,j+1}^{k,1}$, $k=1,\ldots,N$. We need the auxiliary points A_k, B_k, T_k, S_k drawn in Fig. 7:

$$A_k=\left(x_i-\frac{h}{2},a_k\right)=\left(x_i-\frac{h}{2},y_j-\frac{h}{2}+\left(k-\frac{1}{2}\right)h^2\right),\quad k=1,\ldots,N,$$

$$B_k=\left(b_k,y_j+\frac{h}{2}\right)=\left(x_i-\frac{h}{2}+\left(k-\frac{1}{2}\right)h^2,y_j+\frac{h}{2}\right),\quad k=1,\ldots,N,$$

$$T_k=(b_k,y_j),\quad S_k=(x_i,a_k),\quad k=1,\ldots,N.$$

Let $\tilde{w}_k$ denote an approximation of u at the point S_k for $k=1,\ldots,N$. Further, we define $\tilde{w}_k$ for $k=1,\ldots,(N+1)/2-1$ by linearly interpolating $w_{i,j}$ and $w_{i,j-1}$, which are the approximations of u at the coarse grid points $x_{i,j}$ and $x_{i,j-1}$, respectively:

$$\tilde{w}_k=\frac{1+(2k-1)h}{2}w_{i,j}+\frac{1-(2k-1)h}{2}w_{i,j-1},\quad k=1,\ldots,\frac{N+1}{2}-1. \tag{3.14}$$

Obviously, $\tilde{w}_{(N+1)/2}=w_{i,j}$. In order to define $\tilde{w}_k$ for $k=(N+1)/2+1,\ldots,N$ we linearly interpolate $w_{i,j}$ and $w_{i,j+1}^{(N+1)/2,1}$ which is the approximation of u at the center of the fine grid cell $\Omega_{i,j+1}^{(N+1)/2,1}$. Then we have

$$\tilde{w}_k=\left(2-\frac{2kh}{1+h}\right)w_{i,j}+\left(\frac{2kh}{1+h}-1\right)w_{i,j+1}^{(N+1)/2,1},\quad k=\frac{N+1}{2}+1,\ldots,N. \tag{3.15}$$

Next we will deal with the approximations at the points T_k, $k=1,\ldots,N$, which we denote by $\tilde{v}_k$. In order to define $\tilde{v}_k$ for $k=1,\ldots,(N+1)/2-1$ we linearly interpolate $w_{i,j}$ and $w_{i-1,j}^{N,(N+1)/2}$ which is the approximation of u at the center of the fine grid cell $\Omega_{i-1,j}^{N,(N+1)/2}$. Then we have

$$\tilde{v}_k=\frac{2kh}{1+h}w_{i,j}+\left(1-\frac{2kh}{1+h}\right)w_{i-1,j}^{N,(N+1)/2},\quad k=1,\ldots,\frac{N+1}{2}-1. \tag{3.16}$$

Obviously, $\tilde{v}_{(N+1)/2}=w_{i,j}$. In order to define $\tilde{v}_k$ for $k=(N+1)/2+1,\ldots,N$ we linearly interpolate $w_{i,j}$ and $w_{i+1,j}$ to obtain

$$\tilde{v}_k=\frac{3-(2k-1)h}{2}w_{i,j}+\frac{(2k-1)h-1}{2}w_{i+1,j},\quad k=\frac{N+1}{2}+1,\ldots,N. \tag{3.17}$$

Please cite this article as: M. Ashyraliyev, et al., On the numerical solution of diffusion–reaction equations with singular source terms, J. Comput. Appl. Math. (2007), doi: 10.1016/j.cam.2007.04.017

We are now ready to set up the finite volume discretization. Integrating (2.16) over $\Omega_{i,j}$ and dividing by the cell volume, we get

$$-\frac{1}{h^2}\int_{\Omega_{i,j}} \Delta u(x,y)\,\mathrm{d}x\,\mathrm{d}y = 0,$$

because the assumption is that Γ does not intersect $\Omega_{i,j}$. Applying the divergence (Gauss) theorem gives

$$-\frac{1}{h^2}\left(\sum_{k=1}^{N}\int_{b_k-h^2/2}^{b_k+h^2/2} u_y\left(x, y_j+\frac{h}{2}\right)\mathrm{d}x - \int_{x_i-h/2}^{x_i+h/2} u_y\left(x, y_j-\frac{h}{2}\right)\mathrm{d}x\right.$$

$$\left.+\int_{y_j-h/2}^{y_j+h/2} u_x\left(x_i+\frac{h}{2}, y\right)\mathrm{d}y - \sum_{k=1}^{N}\int_{a_k-h^2/2}^{a_k+h^2/2} u_x\left(x_i-\frac{h}{2}, y\right)\mathrm{d}y\right) = 0, \tag{3.18}$$

revealing the fact that Γ does intersect $\Omega_{i-1,j}$ and $\Omega_{i,j+1}$. By approximating the integrals with the common midpoint rule, the left-hand side is approximated by

$$-\frac{1}{h^2}\left(h^2\sum_{k=1}^{N} u_y(B_k) - hu_y\left(x_i, y_j-\frac{h}{2}\right) + hu_x\left(x_i+\frac{h}{2}, y_j\right) - h^2\sum_{k=1}^{N} u_x(A_k)\right).$$

We use second-order approximations for the fluxes

$$u_y\left(x_i, y_j-\frac{h}{2}\right) \simeq \frac{w_{i,j}-w_{i,j-1}}{h}, \quad u_x\left(x_i+\frac{h}{2}, y_j\right) \simeq \frac{w_{i+1,j}-w_{i,j}}{h} \tag{3.19}$$

and for other fluxes first-order approximations, namely

$$u_y(B_k) \simeq \frac{2}{h(1+h)}(w_{i,j+1}^{k,1} - \tilde{v}_k), \quad u_x(A_k) \simeq \frac{2}{h(1+h)}(\tilde{w}_k - w_{i-1,j}^{N,k}), \quad k=1,\ldots,N. \tag{3.20}$$

Inserting the flux approximations (3.19)–(3.20), (3.18) becomes

$$-\frac{1}{h^2}\left[w_{i,j-1}+w_{i+1,j}-2w_{i,j}+\frac{2h}{1+h}\sum_{k=1}^{N}(w_{i,j+1}^{k,1}+w_{i-1,j}^{N,k}) - \frac{2h}{1+h}\sum_{k=1}^{N}(\tilde{v}_k+\tilde{w}_k)\right] = 0.$$

Finally, using (3.14)–(3.17), after some calculations we obtain the discretization for the coarse grid cell $\Omega_{i,j}$ which reads

$$-\frac{1}{h^2}\left[\frac{3+h}{4}\left(w_{i,j-1}+w_{i+1,j}\right) - \frac{(3+h)^2}{2(1+h)}w_{i,j} + \frac{2h}{1+h}\sum_{k=1}^{(N+1)/2-1}(w_{i,j+1}^{k,1}+w_{i-1,j}^{N,k})\right.$$

$$\left.+\frac{2h}{1+h}\sum_{k=(N+1)/2+1}^{N}(w_{i,j+1}^{k,1}+w_{i-1,j}^{N,k}) - \frac{1-5h}{2(1+h)}(w_{i,j+1}^{(N+1)/2,1}+w_{i-1,j}^{N,(N+1)/2})\right] = 0. \tag{3.21}$$

Please cite this article as: M. Ashyraliyev, et al., On the numerical solution of diffusion–reaction equations with singular source terms, J. Comput. Appl. Math. (2007), doi: 10.1016/j.cam.2007.04.017

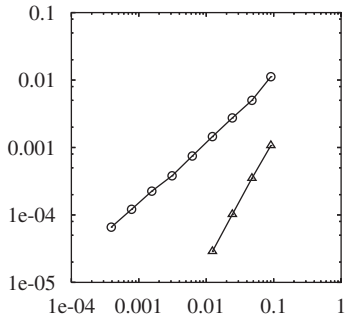

N	$\|u_h - w\|_\infty$	Order
11	1.07×10^{-3}	
21	3.49×10^{-4}	1.73
41	1.02×10^{-4}	1.84
81	2.87×10^{-5}	1.86

Fig. 8. Errors in max norm versus h and convergence orders on the refined grid using the first approach.

In a similar way the discretization for all other cells can be obtained. However, finding the discretization for every cell explicitly in a formula similar to (3.21) is a cumbersome task. To avoid that, we suggest Algorithm 1[3] to generate the discretizations automatically.

Algorithm 1. Algorithm for the finite volume discretization for a single grid cell.

define the neighbouring cells and cell faces
for all cell faces **do**
  compute the fluxes at the cell face centers:
  if the points used for the flux approximation are equally distanced from the cell face center **then**
    use the second-order approximation, similar to (3.19)
  else
    use the first-order approximation, similar to (3.20)
  end if
  if a point used in the flux approximation is not the center of the grid cell **then**
    define the approximation at that point by linearly interpolating approximations at closest grid cells, similar to (3.14)–(3.17)
  end if
end for
compute the finite volume discretization for the cell

Combining it all, we then obtain an $N_c \times N_c$ linear system, where N_c is the total number of cells. If there are N_Γ coarse grid cells intersected by Γ, then $N_c = N_\Gamma(N^2 - 1) + N^2$. Note that, if N_Γ is of order N, then N_c is of order N^3, which means that we have gained one order in complexity compared to an overall uniform refinement.

We have applied the current 2D local refinement method to problem (2.16), (2.17), (2.20) on the unit square $0 \leqslant x, y \leqslant 1$ with Dirichlet boundary conditions. The resulting linear systems were resolved to sufficient accuracy by means of the iterative Bi-CGSTAB method (see [9]) with ILU(0) preconditioning (see [5, p. 294]). For comparison we also include the uniform grid approach in the plot.

Fig. 8 shows the first-order convergence for the uniform grid (o-marks) and second-order convergence for the refined grid approach (△-marks). The table gives more quantitative information for the refined grid approach. We note that for $N = 161$ the number of nonzero entries in the resulting matrix is about 4.2×10^7 which makes it impossible to compute the numerical solution on our processor. However, we clearly see that the convergence order is roughly 2. Still the method is quite expensive because N_c is of order N^3. Below we will therefore present ways to refine the grid such that N_c is of order N^2.

[3] The source codes are available from the first author.

Please cite this article as: M. Ashyraliyev, et al., On the numerical solution of diffusion–reaction equations with singular source terms, J. Comput. Appl. Math. (2007), doi: 10.1016/j.cam.2007.04.017

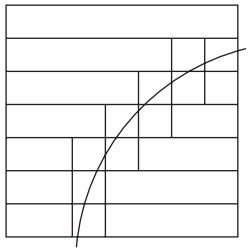

Fig. 9. Refinement of the coarse grid cell intersected by Γ (second approach).

Table 1
Errors and convergence orders on the refined grid using the second approach

N	$\|u_h - w\|_\infty$	Order
11	2.19×10^{-3}	
21	7.52×10^{-4}	1.66
41	2.99×10^{-4}	1.38
81	1.40×10^{-4}	1.12

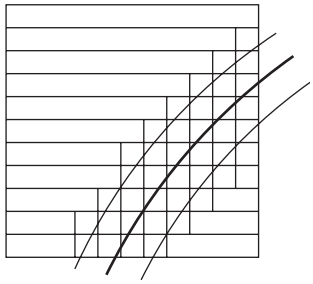

Fig. 10. Refinement of the coarse grid cell intersected by the strip (third approach).

3.2.2. Second approach

In our second approach coarse grid cells intersected by Γ are refined as schematically shown in Fig. 9. In this way Γ intersects only small square cells of size h^2. The idea behind this refinement is that if N_Γ is of order N, then N_c is of order N^2, gaining one order in comparison with the first approach.

For the finite volume discretization on the resulting refined grid Algorithm 1 can be used in a similar way. Table 1 shows errors in the max norm and convergence orders for the new refined grid approach. As we can see, the refinement fails because the convergence order goes down for increasing N. The maximum error in all cases occurs in those cells where we used first-order approximation for flux computation at points at different sides of Γ. Due to the discontinuity of the first derivatives of u across Γ, such approximation causes serious order reduction. In the next section we will examine how to overcome this.

3.2.3. Third approach

As we have seen in the previous section, the first-order approximation for the flux computation at points at different sides of Γ results in order reduction. To achieve a second-order flux approximation we introduce a 2D strip around Γ. In our case, when Γ is the circle, the strip is given by $\{(x, y) : (r-d)^2 \leqslant (x-x_c)^2 + (y-y_c)^2 \leqslant (r+d)^2\}$. Now we can refine the grid in a similar way as it was done in the previous section. Fig. 10 shows schematically the refinement of coarse grid cells intersected by the strip.

Please cite this article as: M. Ashyraliyev, et al., On the numerical solution of diffusion–reaction equations with singular source terms, J. Comput. Appl. Math. (2007), doi: 10.1016/j.cam.2007.04.017

Table 2
Errors and convergence orders on the refined grid using the third approach with $d = \sqrt{2}h^2$

N	$\|u_h - w\|_\infty$	Order
11	1.73×10^{-3}	
21	6.22×10^{-4}	1.58
41	2.09×10^{-4}	1.63
81	6.68×10^{-5}	1.68
161	1.92×10^{-5}	1.82

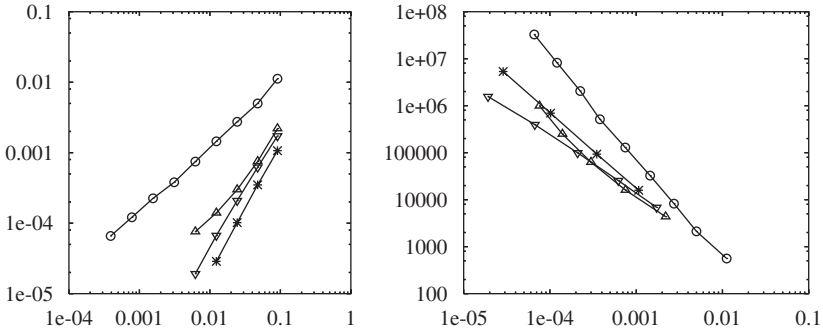

Fig. 11. Errors in max norm versus h (left) and number of nonzero elements in the matrices versus error (right) on the uniform grid (o-marks), on the refined grid using the first approach ($*$-marks), on the refined grid using the second approach ($\triangle$-marks) and on the refined grid using the third approach with $d = \sqrt{2}h^2$ (∇-marks).

For the finite volume discretization on such a refined grid again Algorithm 1 introduced in Section 3.2.1 can be used. Note, that if N_Γ is of order N, then N_c is of order N^2, similar to the second approach. Table 2 shows errors in the max norm and convergence orders for a strip with $d = \sqrt{2}h^2$. As we can see, the convergence order approaches 2 when N increases. Necessary for the strip approach to work is that it is wide enough. Apparently, this holds with $d = \sqrt{2}h^2$, while $d = h^2$ still shows order reduction.

Fig. 11 summarizes all numerical results. As we have already mentioned, only on the refined grids using the first and third approach second-order convergence is obtained. The third approach is favorable due to the smaller number of nonzero entries in the resulting matrix.

3.3. Time-dependent problems

The extension from boundary-value problems to time-dependent problems on a locally refined grid is essentially the same as for the uniform grid approach described in Section 2. Spatial discretization on a locally refined grid also leads to a system of ODEs which can be solved by an appropriate time integrator. For reaction–diffusion time-dependent problems with nonstiff reactions, by using IMEX schemes for time discretization, reaction terms can be treated explicitly and the Jacobian matrices consist of entries from the spatial discretization of the diffusion operator. For time-dependent problems the numerical stability depends on the spectrum of the matrix and the solution of the resulting linear system on the condition number. So, the matrix resulting from spatial discretization is of importance. Here we give condition numbers and spectral radii for the matrices in the uniform and refined grid case using the third approach with $d = \sqrt{2}h^2$. The second and third column in Table 3 give the condition numbers C_{uni} and the spectral radii ρ_{uni}, respectively, for the matrices in the uniform grid approach. The fourth and fifth column give the condition numbers C_{ref} and the spectral radii ρ_{ref}, respectively, for the matrices in the refined grid approach before ILU(0) preconditioning. The last column gives the condition numbers C^*_{ref} for the matrices in the refined grid approach after ILU(0) preconditioning. As we can see, the spectral radii are of the same order implying that the same stability constraints hold with respect to time-stepping. But the condition numbers in the local grid refinement case are much larger than in the uniform grid case. By applying the ILU(0) preconditioner, we get condition numbers significantly smaller than in the uniform grid approach.

Please cite this article as: M. Ashyraliyev, et al., On the numerical solution of diffusion–reaction equations with singular source terms, J. Comput. Appl. Math. (2007), doi: 10.1016/j.cam.2007.04.017

Table 3
Condition numbers and spectral radii of matrices in uniform ($k = 2$) and refined ($k = 1$) grid cases

N	C_{uni}	ρ_{uni}	C_{ref}	ρ_{ref}	C^*_{ref}
11^k	8.63×10^3	1.17×10^5	1.64×10^5	1.11×10^5	1.35×10^3
21^k	1.15×10^5	1.55×10^6	3.40×10^6	1.47×10^6	6.08×10^3
41^k	1.66×10^6	2.26×10^7	8.54×10^7	2.14×10^7	3.69×10^4
81^k	2.54×10^7	3.44×10^8	2.49×10^9	3.27×10^8	2.63×10^5
161^k	3.96×10^8	5.37×10^9	7.65×10^{10}	5.11×10^9	2.00×10^6

4. Concluding remarks

In this paper we have numerically studied 1D and 2D elliptic and parabolic problems with singular source terms. Such sources do contain or are defined by a Dirac delta function expression on a lower dimensional surface. By this type of singularity, solutions are not differentiable across these surfaces which hampers the spatial discretization. We have examined the common second-order finite volume technique which in itself provides a natural spatial discretization for elliptic and parabolic problems having this type of singular source terms. However, the lack of differentiability causes order reduction, that is, on a uniform grid the convergence rate reduces from two to one in the maximum norm. To overcome this deficiency, we have examined discretization on a number of special locally refined grids, in 1D analytically and in 2D experimentally. We have shown that by an appropriate locally refined grid the maximum norm second-order convergence can be restored, and in such a way that the number of nonzero entries in the resulting difference matrix is of the same order as on the uniform grid. For time-dependent problems with nonstiff reactions integrated with IMEX methods the matrices resulting from spatial discretization of diffusion terms is of importance. We have shown that the local grid refinement approach does not change the spectral radii of these matrices, and thus the time-stepping constraints, but does increase the condition numbers. This problem can be circumvented by preconditioning the matrices. Of course, in 2D it is unavoidable that the sparsity pattern does change and that we lose the simple 5-point structure of the uniform grid. This will unavoidably increase solution costs, whether a direct sparse solver or a preconditioned iterative solver will be used. Therefore, despite the fact that restoring second-order maximum norm convergence is of clear interest in its own, from the practical point of view we advise the locally refined grid technique only when higher accuracy levels are wanted. Fig. 11 (right plot) illustrates this nicely. In our tests the first-order convergent uniform grid solution is still computed faster up to modest accuracy levels.

Acknowledgments

We acknowledge support from the Dutch BSIK/BRICKS project and from NWO's 'Computational Life Science' program, projectnr. 635.100.010.

References

[1] M.D. Greenberg, Application of Green's Functions in Science and Engineering, Prentice-Hall, Englewood Cliffs, NJ, 1971.
[2] E. Hairer, C. Lubich, G. Wanner, Geometric Numerical Integration. Structure Preserving Algorithms for Ordinary Differential Equations, Springer Series in Computational Mathematics, vol. 31, Springer, Berlin, 2002.
[3] W. Hundsdorfer, J.G. Verwer, Numerical Solution of Time-Dependent Advection–Diffusion–Reaction Equations, Springer Series in Computational Mathematics, vol. 33, Springer, Berlin, 2003.
[4] J.M. Ortega, W.C. Rheinboldt, Iterative Solution of Nonlinear Equations in Several Variables, New York, London, 1970.
[5] Y. Saad, Iterative Methods for Sparse Linear Systems, second ed., SIAM, Philadelphia, 2003.
[6] N.M. Temme, Special Functions, an Introduction to the Classical Functions of Mathematical Physics, Wiley, New York, 1996.
[7] N.M. Temme, Personal communication, 2005.
[8] A.-K. Tornberg, B. Engquist, Numerical approximations of singular source terms in differential equations, J. Comput. Phys. 200 (2004) 462–488.
[9] H.A. van der Vorst, BI-CGSTAB: A fast and smoothly converging variant of BI-CG for the solution of nonsymmetric linear systems, SIAM J. Sci. Statist. Comput. 13 (2) (1992) 631–644.

Please cite this article as: M. Ashyraliyev, et al., On the numerical solution of diffusion–reaction equations with singular source terms, J. Comput. Appl. Math. (2007), doi: 10.1016/j.cam.2007.04.017